On the Interesting Optical Properties of Highly Transparent, Thermally Stable, Spin-Coated Polystyrene/Zinc Oxide Nanocomposite Films

P. P. Jeeju, S. Jayalekshmi

Division for Research in Advanced Materials, Department of Physics, Cochin University of Science and Technology, Kochi, Kerala, India

Received 7 June 2010; accepted 16 August 2010
DOI 10.1002/app.33188
Published online 24 November 2010 in Wiley Online Library (wileyonlinelibrary.com).

ABSTRACT: In the present work, polystyrene/zinc oxide (PS/ZnO) nanocomposite films are prepared by simple mixing followed by film deposition, using spin-coating technique. Although there are a few reports on the UV-shielding properties of PS/ZnO nanocomposite films, these reports deal with rather thick films obtained by solution casting. Spin coating is a more advantageous technique where one can control the film thickness by suitably adjusting the viscosity of the solution and the spinning speed and get homogeneous films with thickness around a few hundreds of nanometers. These aspects provide the motivation for the present work where emphasis is given to investigating the optical properties of PS/ZnO nanocomposite films obtained by spin coating and analyzing the effects of each component of the composite (PS/ZnO) on the properties of the other. The nanocomposite films are found to be highly transparent throughout the visible region and the thermal stability is better compared with PS. The optical absorption of the composite films in the UV region is quite high, and this aspect highlights the prospects of applications of these films in UV shielding. The PS matrix brings about considerable surface modification of ZnO nanoparticles, resulting in the reduction of defect states within ZnO and facilitating sharp, near band edge photoluminescence emission. © 2010 Wiley Periodicals, Inc. J Appl Polym Sci 120: 1361–1366, 2011

Key words: nanocomposite; matrix; UV shielding; surface modification; spin coating

INTRODUCTION

Recently much attention has been given to studies on the organic/inorganic nanocomposite materials, which exhibit a host of interesting optical and electrical properties. Combining organic and inorganic materials result in composites, which inherit the properties of both organic and inorganic components, thus creating scope for extensive applications in many areas. Furthermore, improvements of the physical properties are achieved at very low loadings, compared with micron-sized fillers.[1] Among the many inorganic materials, ZnO is specifically interesting, owing to its direct band gap (Eg = 3.37 eV), large room temperature exciton-binding energy (60 meV),[2] and variety of application fields such as solar cells,[3] gas sensors,[4,5] varistors,[6] acoustic and luminescent devices, etc.[7–9] Another advantage is that ZnO can be synthesized through wet chemistry, which offers a potential viable route to achieve uniform dispersion in polymer matrices through simple mixing. As the size decreases, the semiconductor nanocrystals can have mechanical, optical, electric, and thermal properties quite different from the bulk.[10] It is believed that the unique characteristics of the nanocomposites may also give rise to new opportunities for functional polymer/semiconductor nanocomposites.[11]

Polystyrene (PS) is a transparent thermoplastic material, which is in solid (glassy) state at room temperature but flows if heated above its glass transition temperature and becomes solid again when cooled. Introduction of ZnO filler into polymeric matrices can modify the optical (shielding from UV radiation), electrical, and mechanical properties.[12–14] In the present study, PS/ZnO nanocomposite samples have been prepared by mixing ZnO powder well in PS solution using ultrasonication. Highly transparent thin films of this composite are then obtained by spin-coating technique. Although there are a few reports on the synthesis and various properties of PS/ZnO nanocomposites,[15,16] there are no detailed studies on the optical characterization of PS/ZnO nanocomposite films prepared by spin-coating technique. The present work is an attempt to investigate in detail the optical absorption and photoluminescence (PL) in these spin-coated nanocomposite films and see how the presence of each

Correspondence to: S. Jayalekshmi (jayalekshmi@cusat.ac.in).

component (PS/ZnO) in the nanocomposite is influencing the properties of the other.

EXPERIMENTAL

Sample preparation

Potassium hydroxide (0.1*M*) was dissolved in 200 mL methanol. This solution was heated to 60°C under reflux and stirring. To this solution, zinc acetate dehydrate (0.1*M*) was added. This mixture was kept for 2 hours under the same conditions during which time precipitation was observed to start. After stirring, the system was cooled to 20°C. The precipitate was filtered and washed with hexane and isopropyl alcohol. The filtrate was dried in an oven at 60°C for 5 hours. The white powder obtained was detected to be pure, nanosized ZnO by X-ray diffraction spectra (XRD) analysis. The PS/ZnO nanocomposite solution was prepared by adding ZnO powder into PS solution in toluene, and the mixture was stirred for 2 hours and then sonicated for 5 minutes. This solution was used to prepare thin films by spin coating on ultrasonically cleaned and optically flat glass substrates (Spin 150). Films with three different weight% of ZnO (5%, 10%, and 20%) were prepared. For reference, PS films were also prepared by spin coating, using the solution of PS in toluene.

Characterization

Field emission scanning electron microscopy (FESEM) images were obtained using a HITACHI SU 6600 Microscope with an accelerating voltage of 20 kV. The surfaces of the ZnO nanoparticles and nanocomposite films were studied using FESEM.

XRD were taken on a Rigaku X-ray Diffractometer with Cu-Kα (1.5418 A°) radiation operating at 30 kV and 20 mA. Scanning was carried out in the 2θ range from 10°–70° at a scan speed of 2° per minute.

Fourier transform infrared (FT-IR) spectra of the samples were obtained with AVTAR 370 DTGS FT-IR spectrophotometer in the wave number range 400–4000 $cm^{-1.}$

Thermo gravimetric analysis (TGA) of the nanocomposite samples was carried out on a Diamond TG/DTA instrument. Samples were heated to 800°C at a scan rate of 10°C per minute in nitrogen atmosphere.

UV-visible absorption spectra were recorded on a Jasco-V 500 spectrophotometer in the wavelength range 190–700 nm.

The PL emission spectra of the samples were obtained with Fluoromax-3 Spectrofluorimeter using Xe lamp as excitation source under an excitation at 325 nm.

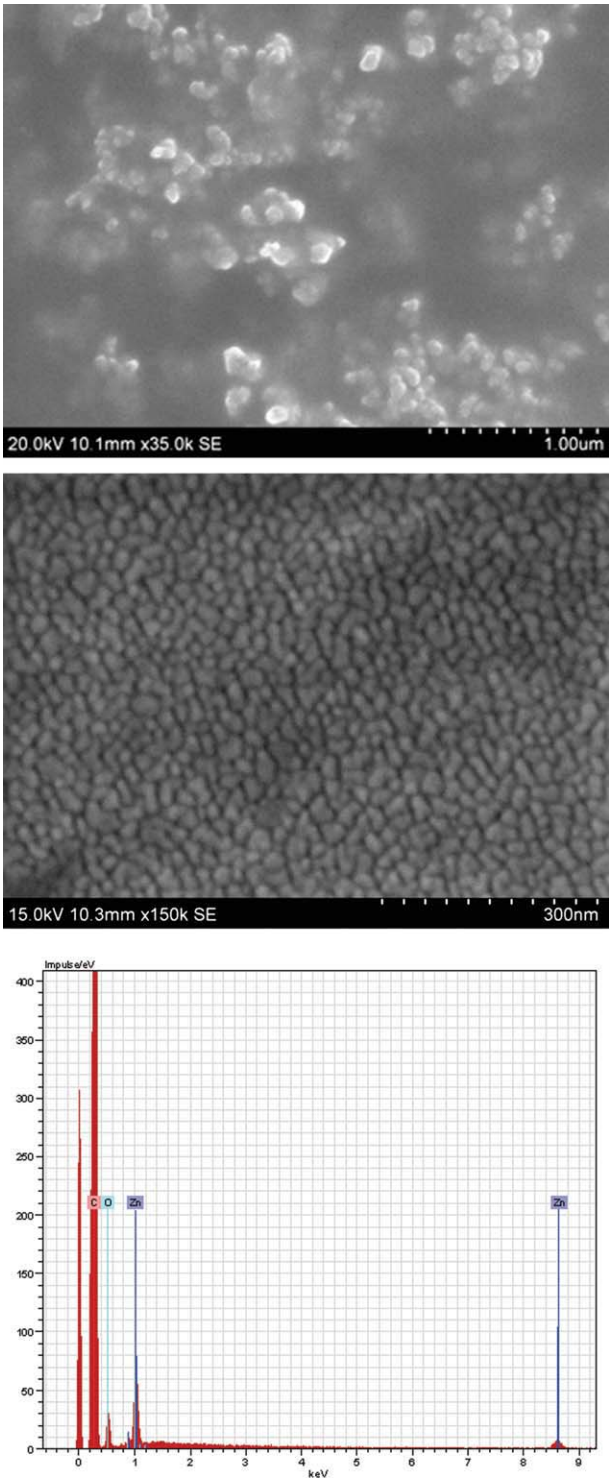

Figure 1 FESEM image of (A) ZnO nanoparticles (B) PS/ZnO nanocomposite film with 10 wt% of ZnO, and (C)The EDS pattern of PS/ZnO nanocomposite. [Color figure can be viewed in the online issue, which is available at wileyonlinelibrary.com.]

RESULTS AND DISCUSSION

FESEM images of ZnO nanoparticles and PS/ZnO nanocomposite film with 10 wt% ZnO are shown in Figure 1(A,B). ZnO nanoparticles (average size,

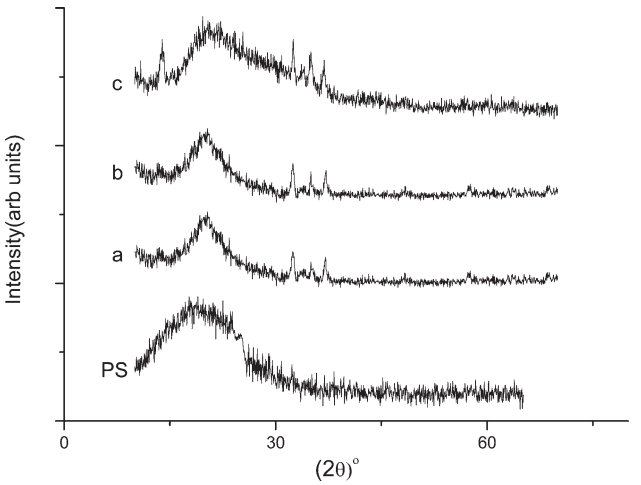

Figure 2 XRD patterns of PS and PS/ZnO composite films (a, b, and c—PS/ZnO composite films with 5, 10, and 20 wt% of ZnO, respectively).

10 nm) are homogeneously dispersed in the PS matrix. The efficiency of nanoparticles in improving the properties of the polymer material is primarily determined by the degree of dispersion in the matrix. These nanostructured ZnO in the polymer can change the thermal and optical properties of the composite. The size of the ZnO nanoparticles in the PS matrix corresponds to that of primary particles, except a very few agglomerates. The energy dispersive spectrum (EDS) data clearly indicates the presence of ZnO in the PS matrix [Fig. 1(C)].

The XRD patterns (Fig. 2) show a broad noncrystalline peak of PS and sharp and intense diffraction peaks of ZnO. The diffraction peaks corresponding to (100), (002), (101), (102), (110), (103), and (112) planes indicate the hexagonal structure of ZnO.

The broadening of the XRD peaks indicates the formation of nanosized particles in the prepared sample. The presence of ZnO produces neither new peaks nor peak shifts with respect to PS showing that nano ZnO filled PS composites consist of two phase structures.

Figure 3 shows the FT-IR spectra of ZnO, PS, and PS/ZnO nanocomposites. The spectrum of the nanocomposite exhibits the characteristic absorption bands corresponding to polymeric groups and ZnO. In the spectrum of ZnO, the bands observed at 424, 453, and 527 cm^{-1} are assigned to Zn-O vibrations[17–19] out of which the bands at 453 and 527 cm^{-1} are present in the PS/ZnO composite spectrum confirming the presence of ZnO in the composite. The three bands centered at 1338, 1412, and 1572 cm^{-1} observed in the ZnO spectrum are attributed to the stretching vibration of C = O, C = C, and C-H groups in acetate species. The characteristic vibration bands of aromatic C = C of styrene units are observed at 1452, 1493, and 1601 cm^{-1} in the spectra of PS and PS/ZnO but the relative intensity of these peaks in PS/ZnO has slightly changed. The peaks due to the adsorbed acetate species cannot be clearly distinguished in the PS/ZnO spectra. This could be due to the presence of the PS matrix in which the ZnO nanoparticles are dispersed. The PS matrix can bring about considerable surface modification of the ZnO nanoparticles by eliminating most of the adsorbed species on the surface. That is why the peaks due to the adsorbed species on the surface are not clearly seen in the spectrum of the composite. The changes in the relative intensities of the bands in the region 1500 cm^{-1} in the composite could be due to the minute presence of adsorbed species on the surface of the ZnO nanocrystals. The bands centered at 2924 and 2850 cm^{-1} observed in PS and PS/ZnO spectra are assigned to the asymmetric and symmetric stretching vibrations of -CH_2, respectively. The absorption bands corresponding to aromatic C-H stretching are observed in the range 2900-3200 cm^{-1}. Because the characteristic bands of PS and ZnO are both observed in the PS/ZnO spectrum, it is clear that ZnO is well dispersed in the PS matrix.

The TGA curves of PS and PS/ZnO nanocomposites are shown in Figure 4 and the TGA data are summarized in Table I. The presence of the nanosized ZnO increases the degradation temperature of the polymer composite. The degradation onset temperature (T_{onset}) of PS/ZnO composite, measured as the temperature required for % degradation is higher than that of pure PS beyond 10% degradation. $T_{0.1}$, $T_{0.3}$...$T_{0.9}$ denote the temperatures for 10%, 30%...90% degradation in weight, respectively (Table I). The composite is more thermally stable compared with PS.

The UV-visible absorption spectra of PS and PS/ZnO composite films are shown in Figure 5. Pure PS

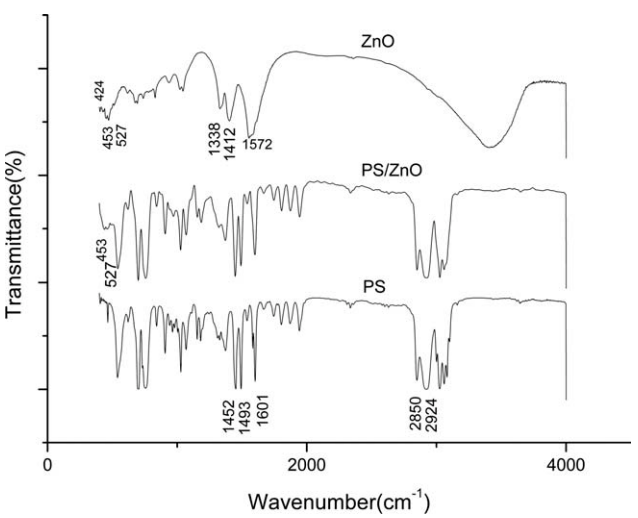

Figure 3 FT-IR spectra of ZnO, PS, and PS/ZnO nanocomposite.

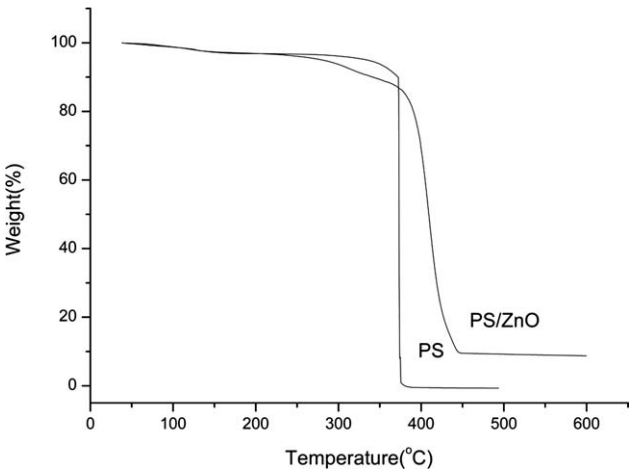

Figure 4 TGA curves of PS and PS/ZnO nanocomposite.

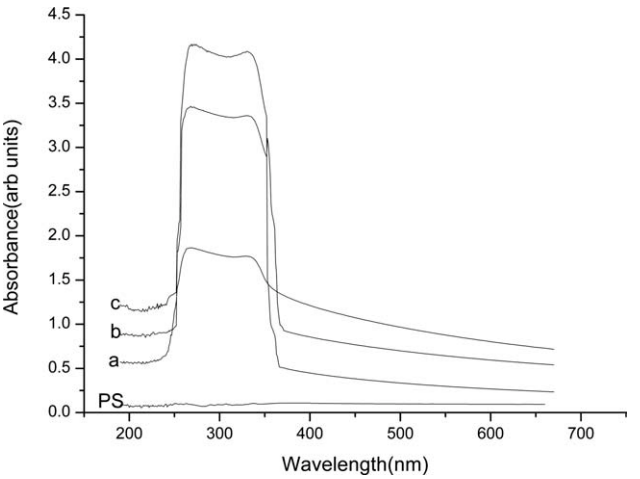

Figure 5 UV-visible absorption spectra of PS and PS/ZnO composite films (a,b, and c—PS/ZnO composite films with 5, 10, and 20 wt%, respectively).

film does not show appreciable UV absorption, and there is only a broad, less intense absorption band centered around 385 nm. For the composite films, an absorption window is found in the range 240-365 nm, and the intensity of UV absorption increases sharply with increase of ZnO content in the composite. Furthermore, the absorption peak wavelength of the composite films are substantially blue shifted relative to that of the bulk ZnO ($\sim$ 373 nm) due to the strong confinement effect.[20] The thicknesses of the PS and PS/ZnO nanocomposite films are measured using the thickness profiler (Dekdak 6*M* Stylus Profiler). The film thickness is found to lie in the range 0.8 to 1 μm for all the films investigated in the present work. In this thickness range, the spin coated films are also found to be homogeneous. In a recent work by Yao Tu et al.[15] PS/ZnO nanocomposite films are shown to exhibit quite high UV-shielding efficiency with the absorption of 99% of UV radiation in the wavelength range between 200 and 360 nm. In that work, however, the film thickness is very high, which is about 360 μm; the ZnO used is not pure, but ligand modified and the technique of film deposition is solution casting where one cannot have good control over the film thickness. In the present work, about 1 μm thick spin-coated film of PS/ZnO nanocomposite film is showing about 90% UV absorption in the wavelength range from 240 to 365 nm with 20% of ZnO loading in the composite. These films are highly transparent in the visible range and offer prospects of application as transparent UV radiation protectors in the wavelength range from 240 to 365 nm. The presence of ZnO nanoparticles, thus, enhances the UV absorption of the composite films and modifies the overall optical behavior of PS films.

TABLE I
TGA Data of PS and PS/ZnO Nanocomposites

	$T_{0.1}$	$T_{0.3}$	$T_{0.5}$	$T_{0.7}$	$T_{0.9}$
PS	368	375	375	375	375
PS/ZnO	330	400	409	417	440

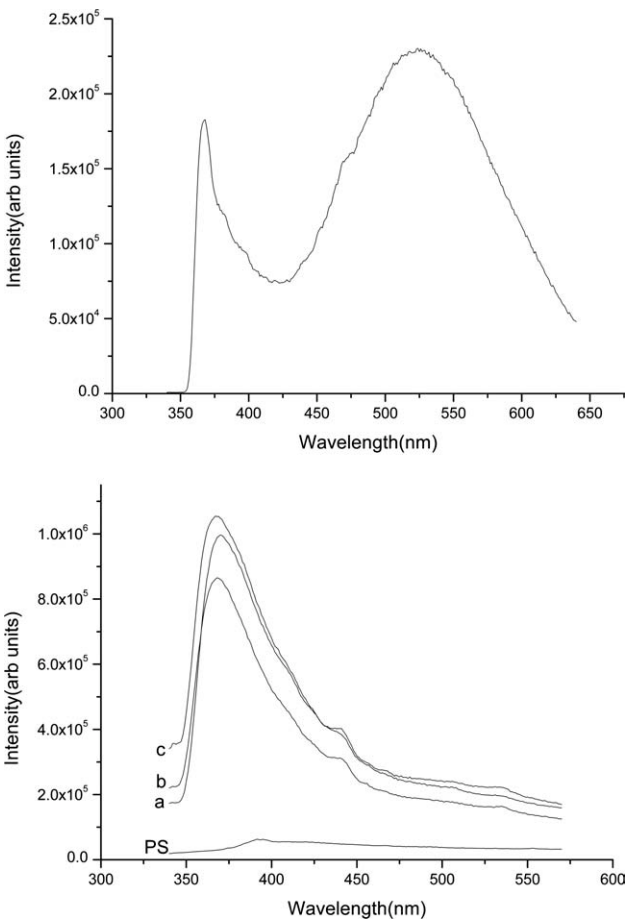

Figure 6 PL emission spectra of (i) ZnO and (ii) PS and PS/ZnO nanocomposite films (a, b and c—PS/ZnO composite films with 5,10, and 20 wt% of ZnO, respectively).

The PL emission spectra of ZnO and PS/ZnO nanocomposites are shown in Figure 6. The PL spectrum of ZnO depicts a sharp intense emission peak at 367 nm along with a broader but more intense emission peak in the longer wavelength side centered around 530 nm. A kink is also observed in the blue region around 450 nm. Pure PS film does not show any luminescence emission in this region as seen from the PL spectrum. The broad PL band at around 530 nm has actually been reported in bulk ZnO as well as in ZnO quantum dots by many researchers.[21–24] But the origin of this broad luminescence is not fully established. The composite films show intense luminescence emission centered around 367 nm in the UV region and intensity of this emission peak is found to increase with increase of ZnO content in the composite. The intensity of the broad luminescence observed around 530 nm relative to that of the UV luminescence decreases considerably and is almost quenched in the composite films. The kink observed in the blue region of the ZnO spectrum becomes more visible in the spectra of the composite films.

The green emission in ZnO originates mainly from the deep surface traps, which can almost be removed via surface passivation by PS. The kink in the blue region of the PL spectrum of ZnO is not much observable because of the presence of the broad intense green emission. But, this kink is more prominent in the Pl spectra of the composite due to the considerable lowering of PL intensity in the green region. The suppression of green luminescence is due to the surface modification of ZnO nanocrystals by the polymer whereby the deep surface traps are almost removed.[22] The observed blue emission in ZnO and the PS/ZnO composite arises from the presence of acetate impurities incorporated in ZnO, possibly during the synthesis process; from the precursor zinc acetate. In ZnO, it appears only as a kink mainly because of the presence of the broad and intense emission in the green region. Because the green emission is almost suppressed in the composite, the blue emission appears more pronounced. The intensity of the blue emission increases with increase in the ZnO content in the composite, and this observation also points toward the presence of acetate impurities on the ZnO surface, as the possible reason for this emission. The FT-IR spectra of the ZnO powder and PS/ZnO composite also support the presence of acetate impurities incorporated onto ZnO.

CONCLUSIONS

Transparent films of PS/ZnO nanocomposites are prepared by spin coating with thickness around 1 μm where pure ZnO nanoparticles without surfactants are used. Good surface functionalization of ZnO with the polymer facilitates the incorporation of these particles into the polymer matrix. The nanocomposite films exhibit good UV-shielding properties in the wavelength range from 240 to 365 nm, where a UV absorption window of about 125 nm has been observed. The UV absorption of about 90% observed in the present work can be further enhanced by increasing the film thickness and also by using nontoxic surfactants to achieve further surface modification of pure ZnO. This could also result in the extension of the wavelength range of high UV absorption down to 180 nm. The present work offers ample scope for further studies with spin coated films of PS/ZnO because the various parameters of spin coating can be suitably optimized to get desired results. Another highlight of the present work is the observation that the PS matrix itself brings about considerable surface modification of ZnO by almost removing the trap and impurity levels in ZnO. This effect is manifested as the quenching of the trap level related PL emission around 530 nm in the PS/ZnO composite films. In the composite films the emission in the UV region is observed to have much higher intensity. The surface modification of ZnO by the polymer matrix, thus, almost quenches the emission in the visible region and confines the PL emission to the near band edge emission.

One of the authors, Jeeju is grateful to University Grants Commission for providing Teacher Fellowship. The authors acknowledge SEM center, NIT Calicut for the FESEM and STIC, CUSAT Kochi for the FT-IR and TGA measurements.

References

1. Alexandre, M.; Dubois, P. Mater Sci Eng 2000, 28, 1.
2. Yi, G.-C.; Wang, C.; Park, W. I. Semicond Sci Tech 2005, 20, S22.
3. Beek, W. J. E.; Wienk, M. M.; Janssen, R. A. J. J Mater Chem 2005, 15, 2985.
4. Sahay, P. P. J Mater Sci 2005, 40, 4383.
5. Jiaqiang, X.; Yuping, C.; Daoyong, C.; Jianian, S. Sensor Actuat B Chem 2006, 113, 526.
6. Kong, L.; Li, F.; Zhang, L.; Yao, X. J Mater Sci Lett 1998, 17, 769.
7. Hao, X. T.; Zhu, F. R.; Ong, K. S.; Tan, L. W. Semicond Sci Tech 2006, 21, 48.
8. Shih, W. C.; Wu, M. S. J Cryst Growth 1994, 137, 319.
9. Radovanovic, R. V.; Norberg, N. S.; McNally, K. E.; Gamelin, D. R. J Am Chem Soc 2002, 129, 15192.
10. Alivisatos, A. P. Science 1996, 271, 933.
11. Sheng, W. C.; Kim, S.; Lee, J.; Kim, S. W.; Jensen, K.; Bawendi, N. G. Langmuir 2006, 22, 3782.
12. Lee, J.; Bhattacharyya, D.; Easteal, A. J.; Metson, J. B. Curr Appl Phys 2008, 8, 42.
13. Dong, W. C.; Byoung, C. K. Polym Adv Technol 2005, 16, 846.
14. Erjun, T.; Shaoying, D. Colloid Polym Sci 2009, 287, 1025.
15. Yao, T.; Li, Z.; Yi Zheng, J.; Chao, G.; Zhi Zhen, Y.; Ye Feng, Y.; Qing Ling, W. J Mater Chem 2010, 20, 1594.
16. Tang, E. J.; Liu, H.; Sun, L. M.; Zheng, E. L.; Cheng, G. X. Eur Polym Mater 2007, 43, 4210.

17. Sumetha, S. Science Asia 2008, 34, 031.
18. Yong, J. K.; Kyoung, H. K.; Chang, S. L.; Kwang, B. S. J Ceram Process Res 2002, 3, 146.
19. Siddheswaran, R.; Sankar, R.; Ramesh Babu, M.; Rathnakumari, M.; Jayavel, R.; Murugakoothan, P.; Sureshkumar, P. Cryst Res Technol 2006, 41, 446.
20. Haase, M.; Weller, H.; Henglein, A. J Phys Chem 1988, 92, 482.
21. Gong, V.; Gertrude, T. A.; Neumark, F.; Stephen O'Igor, L. Nanoscale Res Lett 2007, 2, 297.
22. Guo, L.; Yang, S.; Yang, C.; Yu, P.; Wang, J.; Ge, W.; Wong, G. K. L. Appl Phys Lett 2000, 76, s2901.
23. Wu, L.; Wu, Y.; Pan, X.; Kong, F. Opt Mater 2006, 28, 418.
24. Zhang, S. B.; Wei, S. H.; Zunger, A. Phys Rev B 2001, 63, 075205.